Fracture Mechanics of Concrete Structures,
Proceedings FRAMCOS-2, edited by Folker H. Wittmann,
AEDIFICATIO Publishers, D-79104 Freiburg (1995)

APPLICATION OF FRACTURE MECHANICS TO OPTIMIZE REPAIR MORTAR SYSTEMS

G. Martinola and F.H. Wittmann,
Laboratory for Building Materials,
Swiss Federal Institute of Technology Zurich, Switzerland

Abstract
A comprehensive analysis of the loads acting on an overlay applied on an existing concrete structure is carried out in order to identify the nature of the key parameters. This study is aimed to allow description of the mechanical behaviour of these materials under hygral and thermal loads. Several types of mortar have been characterized with respect to their mechanical behaviour and in particular, their fracture energy. In addition, the hygral diffusion coefficient has been determined. A numerical model to simulate the behaviour of a mortar under drying conditions is used to predict crack formation and debonding. On this basis a systematic optimisation can be carried out.

1 Introduction

The porous structure of concrete interacts with the environment in which an element is placed. The protective effect of the covercrete can be lost by carbonation. Chlorides and other ions may penetrate into the surface near zones. In order to restore the initial state concrete is often removed in these cases. A new layer which may be cast or applied by shotcreting has a different hygral and mechanical history as compared to the substrate.

So far, repair mortars are developed on an empirical basis. Only few attempts exist to study the hygral and thermal loads and the risk for delamination or crack formation in detail.
In this contribution a numerical approach is briefly presented which allows us to analyse stress histories under given boundary conditions. With the help of this model it is possible to predict the time-dependent behaviour of repair layers. An optimization can be carried out by a rigorous parameter study.

2 Qualitative consideration of stresses occuring in a drying system substrate-overlay

After the application of a new cover on old concrete time-dependent deformations take place. Normaly a time dependent moisture distribution is built up and therefore stresses are induced in the overlay substrate system.

The internal and external factors influencing the state of stresses can be classified in the following way :

a.) Internal loads

- Thermal gradients due to the exothermic reaction of hydration
- Chemical shrinkage
- Endogeneous shrinkage
- Swelling caused by shrinkage compensating agents

b.) External loads

- Mechanical loads, static and dynamic
- Eigenstresses due to hygral gradients as a consequence of drying
- Eigenstresses due to thermal gradients as a consequence of external heating or cooling

In Fig. 1 the stress distribution of a drying system of old and new concrete is shown schematically after Haardt (1991).

We can distinguish two failure criteria of the system :

- If the tensile strength f_t of the new concrete is reached, surface cracks in vertical direction 'y' will appear
- If the adhesion of the new mortar with the substrate is surpassed, a "warping effect" will take place : the delamination of the interface will start from free edges.

In reality it is difficult to describe the occuring time-dependent stresses realistically. Numerical methods have to be applied. We have chosen a finite element approach (MARC, 1994). The essentials of the numerical model are described in the following section.

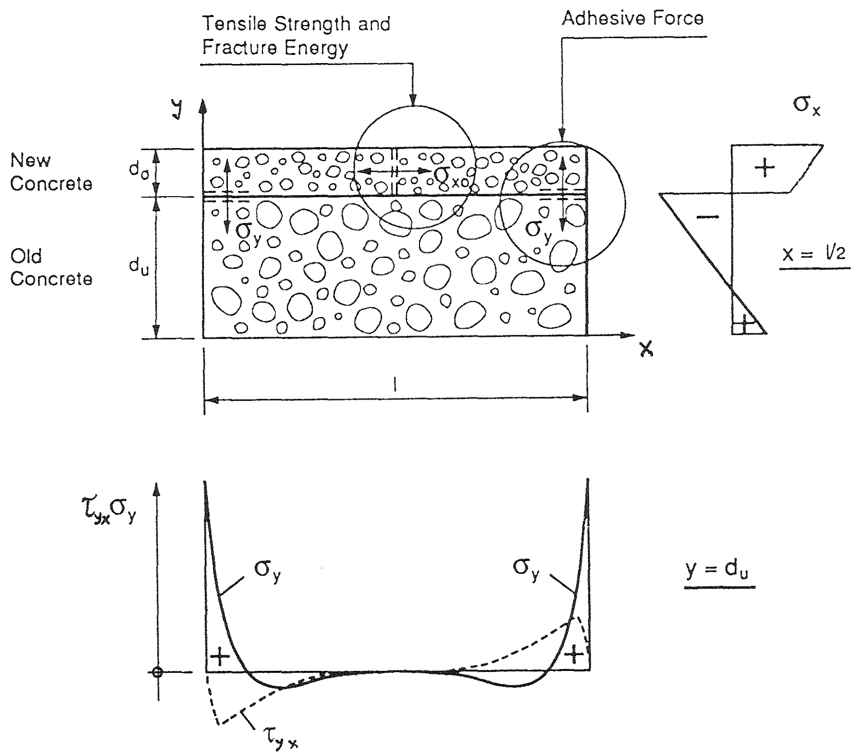

Fig. 1. Stress distribution in a drying concrete repair system according to Haardt (1991)

3 The numerical model

3.1 Moisture transport and moisture distribution

As has been pointed out already a rigorous analysis is most complex. We limit ourselves therefore to the prediction of time-dependent moisture distributions, provoked eigenstresses, and the damage and crack formation.

The moisture transport can be described by the following differential equation as has been shown by Pihalajavaara (1965) and Bazant and Najjar (1971) :

$$\dot{h} = div\left[D(h) \cdot \vec{grad}(h)\right] \tag{1}$$

in which D(h) represents the moisture diffusion coefficient. This value depends strongly on moisture content. D(h) has been determined on the basis of drying experiments by Wittmann et al. (1989). For an analytical approximation an exponential equation can be used.

$$D(h) = a \cdot \exp(b \cdot h) \quad (2)$$

In order to take convective boundary conditions at the surface 's' into consideration, a film coefficient is introduced:

$$q_s = H_F \cdot (h_s - h_a) \quad (3)$$

where q_S is the moisture flux normal to the surface, H_F is the film coefficient, h_a is the ambient humidity and h_S is the relative humidity of the surface. Here a film coefficient of 0.7mm/day has been used

3.2 Stress distribution and crack formation

The moisture distribution can be converted into a strain field with the help of the following equation:

$$\Delta\varepsilon_{d.sh} = \alpha_{d.sh}(h) \cdot \Delta h \quad (4)$$

where $\Delta\varepsilon_{d.sh}$ is the infinitesimal shrinkage strain, Δh is the hygral gradient and $\alpha_{d.sh}(h)$ is the hygral coefficient of shrinkage. This strain field is at the origin of a state of eigenstresses.

Before the tensile strength is reached the material is considered to be linear elastic. The post peak behaviour is described by fracture energy and strain softening. The elastic modulus and the tensile strength are introduced as statistically normal distributed values (see also Sadóuki and Wittmann (1995) and Alvaredo (1994)).

The system of old concrete, interface, and new mortar has been generated by finite elements. A typical example is shown in Fig. 2.

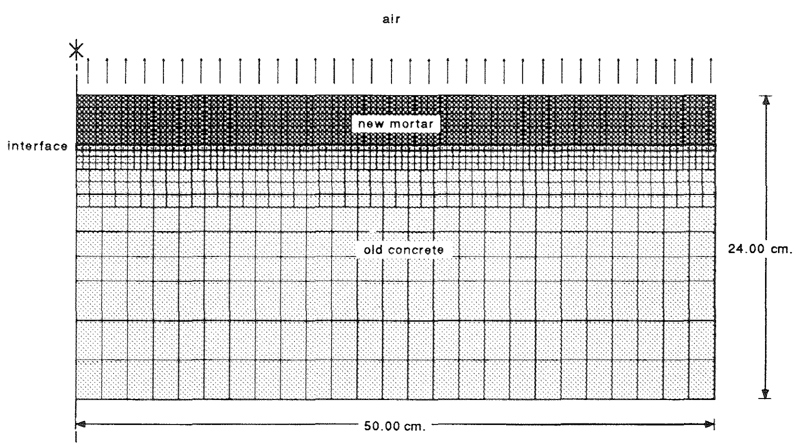

Fig. 2. Shape of the implemented mesh

4 Material parameters needed for the numerical analysis

4.1 Hygral diffusion coefficient

Parameters a and b of equation (2) have been determined by means of an inverse analysis. Measured values of weight loss in a constant humidity served as an experimental basis. For the mortar studied in this project the following value has been obtained:

$$D(h) = 0.022 \cdot \exp(9.48 \cdot h) \tag{5}$$

The assumed functions for mortar, and the concrete substrate are given in Fig. 3.

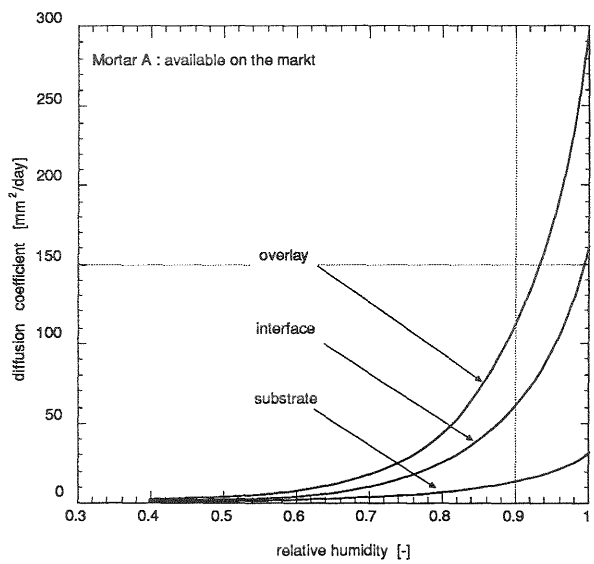

Fig. 3. Hygral diffusity as function of the humidity for mortar, interface and substrate.

4.2 Shrinkage

Hygral shrinkage has been measured in three different relative humidities. The shrinkage function has been extrapolated to obtain approximately the final value. The result is shown in Fig. 4 a.

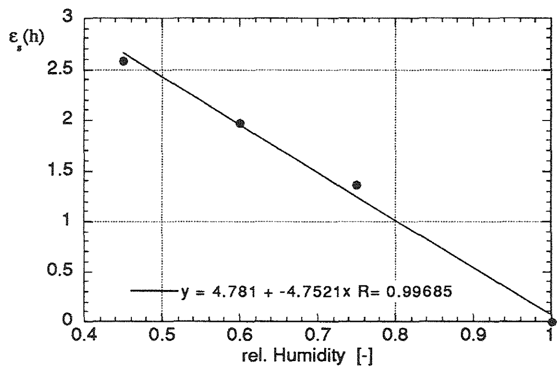

Fig. 4. Final shrinkage of the mortar as function of relative humidity

From these results the hygral coefficient of shrinkage can be obtained.

$$\alpha_{d.sh}(h) = \frac{d\varepsilon^{t\rightarrow\infty}(h)}{dh} \tag{6}$$

As an approximation a constant value can be used: $\alpha = 4.8 \bullet 10^{-3}\ h^{-1}$

4.3 Mechanical Parameters

The elastic modulus has been determined to be 26'000 N/mm2. By means of the wedge splitting test fracture energy and strain softening have been determined (Roelfstra and Wittmann (1986)). Results are shown in Fig. 5.

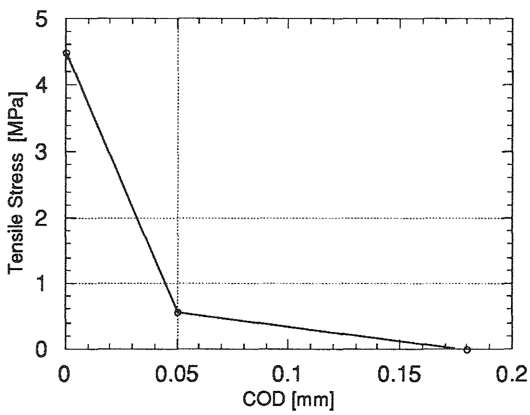

Fig. 5. Strain softening diagram for the investigated mortar

The assumed values for mortar (overlay A), the interface, and the concrete substrate are compiled in Tab. 1.

Table 1. Material properties of the first analysis

	$\alpha_{d.sh}$ (‰.1/h)	G_f (N/m)	E (GPa)	f_t (MPa)	s1 (MPa)	w1 (mm)	w2 (mm)
Overlay A	4.8	161.0	26.0	4.5	0.55	0.05	0.18
Interface	2.8	32.0	28.0	1.0	0.33	0.024	0.12
Substrate	1.3	95.0	33.0	4.0	0.5	0.02	0.2

5 Results

5.1 Moisture distribution

To calculate the time-dependent moisture distribution of an element after the placing of a repair mortar two different initial conditions have been chosen. In the first case, it is assumed that the substrate is old enough to have reached equilibrium with a relative humidity of 50% before the repair measures were started. It is assumed that moisture has been taken up by capillary suction during the removal of the damaged cover by water jet, for example, and the placing of the repair mortar. The assumed step function is given in Fig. 6 a. In the second case, it is assumed that the element was not in hygral equilibrium before the repair measures were started but had reached a relative humidity of 90%. Further, it is assumed that mositure penetrated the substrate by 20 mm only. These initial conditions are shown in Fig. 6 b.

The predicted moisture distribution is shown for both cases after selected drying times in Fig. 6 a and 6 b.

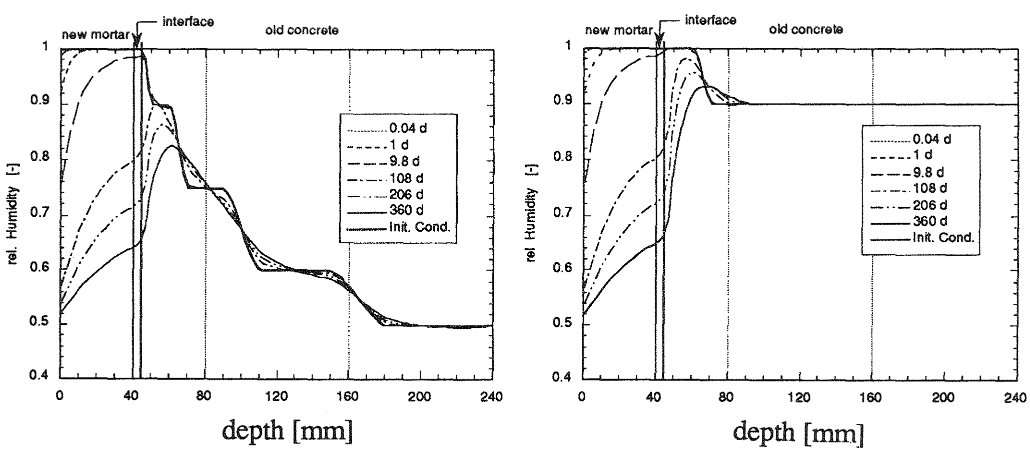

a) b)

Fig. 6. Moisture distribution after different drying times up to one year for two different initial conditions.

In Fig. 7, the moisture distribution of the drying system with the initial conditions of Fig. 6 a, but with a PUR coating on the surface is shown.

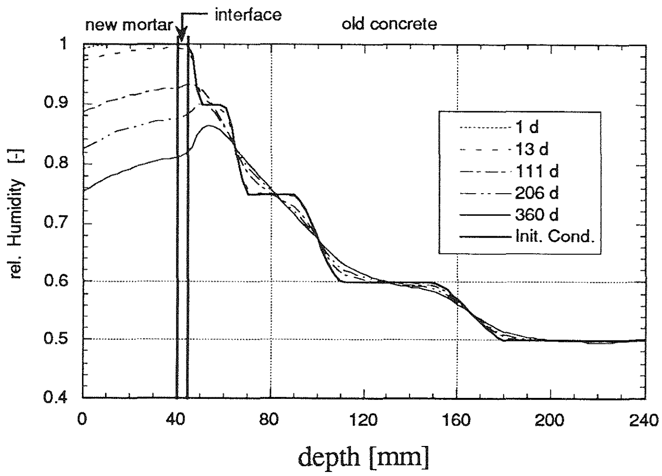

Fig. 7. Moisture distribution of a drying system with surface cover of PUR

5.2 Stress distributions and crack formation

In a first example, the evolution of stresses has been calculated for the hygral initial conditions as shown in Fig. 6 a. Drying takes place in an environment of 50% R.H. As can be seen in Fig. 8, the tensile strength is already overcome after a drying time of 10 days. After 110 days, a crack is formed and the earlier highly stressed surface zones are unloaded.

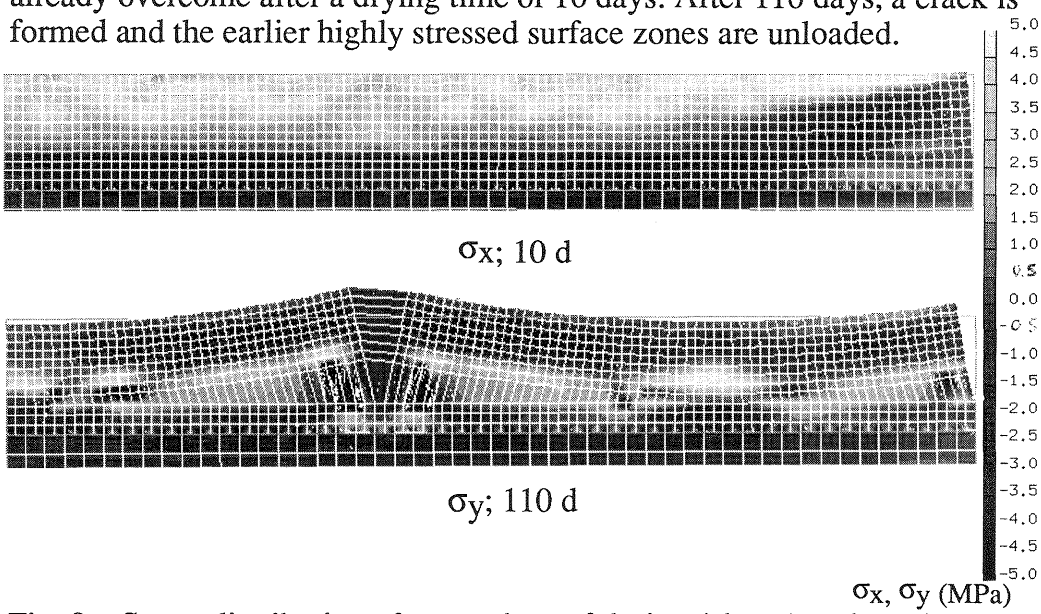

Fig. 8. Stress distribution after ten days of drying (above) and crack formation of a crack after 110 days.

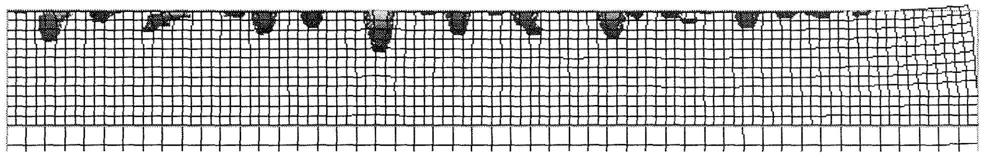

crit. strain 10 d

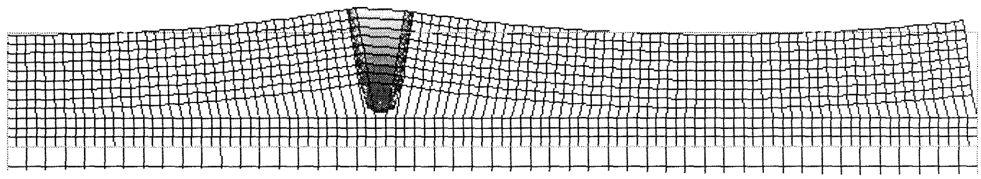

crit. strain 110 d

Fig. 9. Formation of fracture process zones after 10 and 110 days of drying

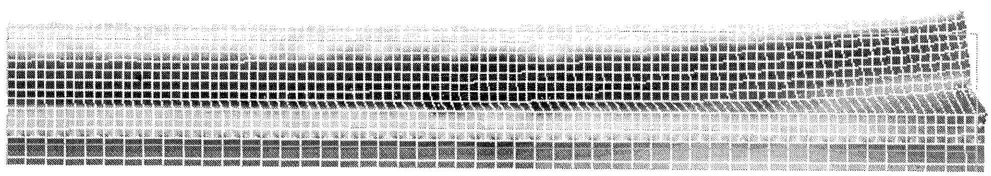

σ_x; 10 d

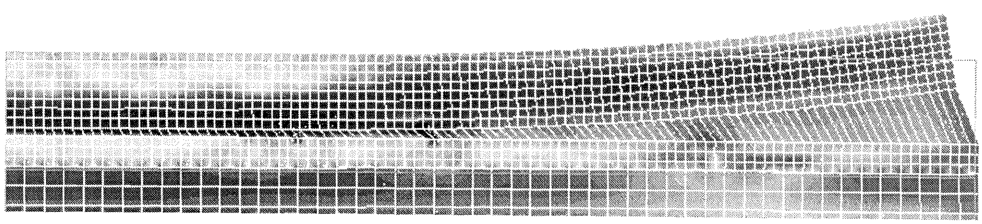

σ_y; 110 d

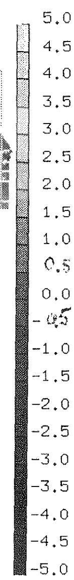

σ_x, σ_y (MPa)

Fig. 10. Stress distribution and crack formation in the overlay and the interface

In Fig. 9, the formation of fracture process zones is visualized for the same conditions as the stress distributions shown in Fig. 8.

For comparison, the stress state of the drying system but with initial conditions as shown in Fig. 6 b are shown in Fig. 10.

In the second example, it is assumed that the interface is much stronger, i.e. the fracture energy is 129 N/m and the tensile strength 4 n/mm^2. After a drying time of 110 days, a crack pattern as shown in Fig. 11 is shown.

It may happen that the overlay is stronger than the old concrete. In order to study this situation it has been assumed that the fracture energy of the concrete substrate is 75 N/m and the corresponding tensile strength 2.5 N/mm^2 only.

The stress and strain distribution in the region near the edge are shown in Fig. 12 for four different durations of drying.

If the surface of the repair mortar is covered by a polymer coating the hygral gradients will be reduced. In the next example, the same system as studied in the first example has been investigated but a PUR coating has been taken into consideration. The moisture distribution has already been shown in Fig. 7. The resulting deformation and stress distribution after 10 days of drying is shown in the upper part of Fig. 13. It can be seen that under these conditions the interface fails near the edge of the system. If, however, the tensile strength of the interface is assumed to be much higher (f_t = 4 N/mm^2) cracking is prevented but higher tensile stresses occur in the overlay. Finally, at a later stage cracks will be formed in the repair mortar as shown in the lower part of Fig. 13.

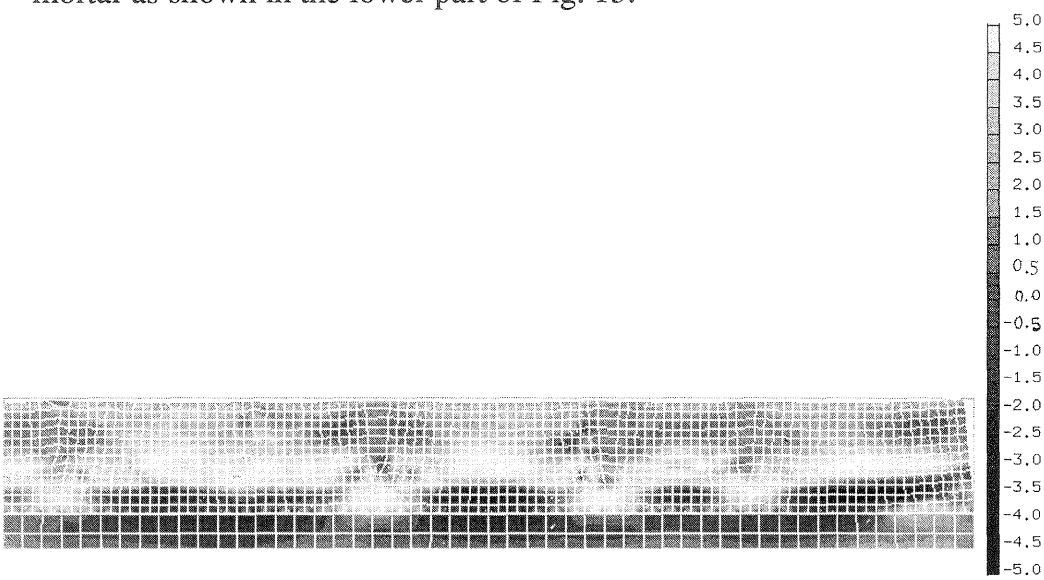

σ_x; 110 d

Fig. 11. Typical crack pattern in an overlay with strong interface.

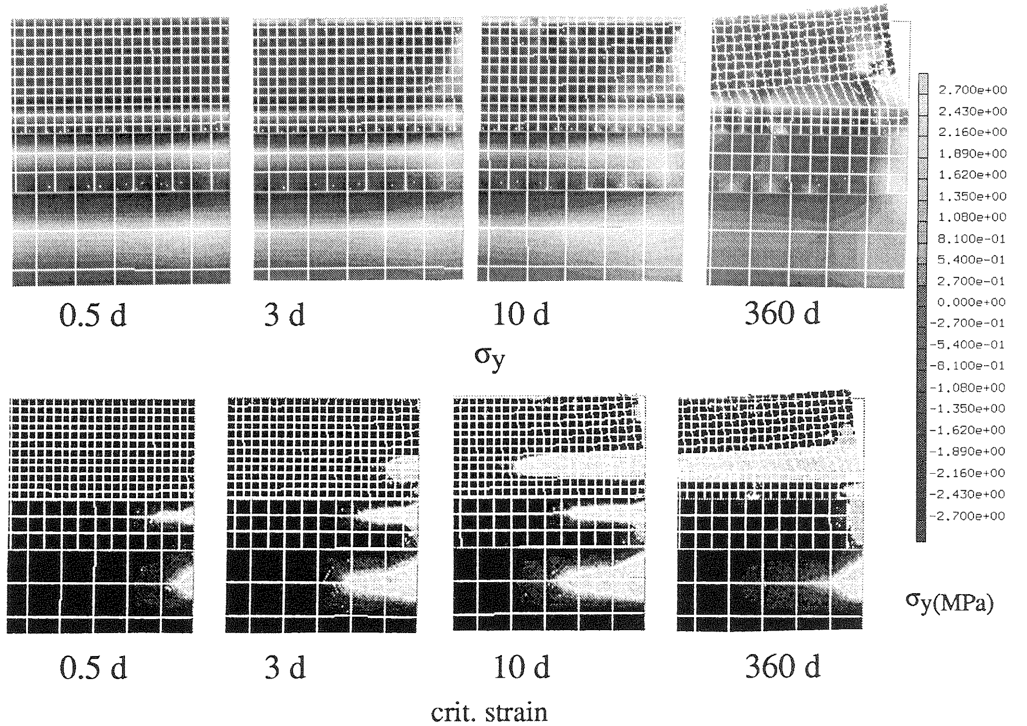

Fig. 12. Stress distribution and crack formation in a week substrate.

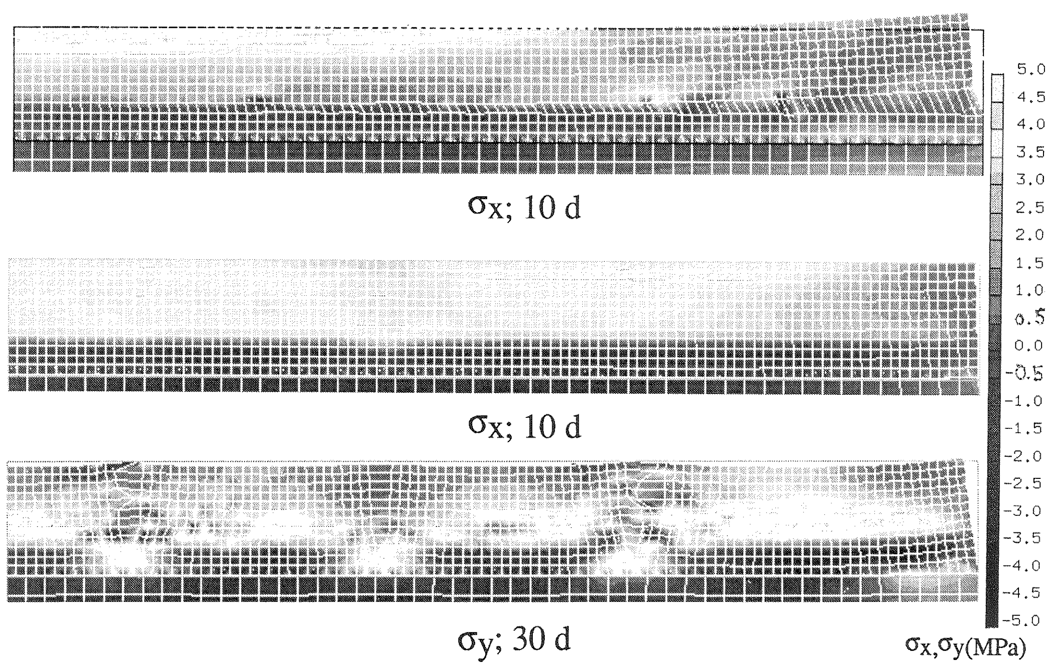

Fig. 13. Stress distribution and crack formation in a PUR coated mortar after different drying times.

It should be pointed out that all these results are mere numerical predictions. The numerical model has still to be validated by a detailed comparison of predictions with experimental findings.

6 Conclusions

A numerical model for the prediction of hygral stresses and crack formation is presented. The most important material properties have to be determined experimentally. When realistic material properties are used different initial and boundary conditions can be taken into consideration. The risk for crack formation for different systems can be estimated by a parametric study. For given initial and boundary conditions properties of a repair mortar can be optimized.

References

Alvaredo, A.M (1994) Drying shrinkage and crack formation. **Building Materials Reports No. 5,** AEDIFICATIO Publishers, Freiburg, Germany.

Bazant, Z.P. and Najjar, L.J. (1971) Drying of concrete as a nonlinear diffusion problem. **Cem. and Concr. Res.**, 1, 461-473.

Haardt, P. (1991) Zementgebundene und kunstoffvergütete Beschichtungen auf Beton, PhD Thesis, Schriftenreihe des Instituts für Massivbau und Baustofftechnologie der Universität Karlsruhe, 13, Germany.

MARC Research Libary, Vol. C : Program Input. Marc Analysis Research Coorparation, Palo Alto (U.S.A.), 1994

Pihalajavaara, S.E (1965) On the main features and methods of investigation of drying and related phenomena in concrete. PhD Thesis, Univ. of Helsinki, Finland.

Roelfstra, P.E. and Wittmann, F.H. (1986) Numerical Method to link strain softening with failure of concrete, in **Fracture toughness and fracture energy of concrete** (ed F.H. Wittmann), Elsevier, Amsterdam.

Sadouki, H. and Wittmann, F.H. (1995) Numerical concrete model applied to investigate size and stability of crack propagation, in this volume.

Wittmann,X., Sadouki, H. and Wittmann, F.H. (1989) Numerical evaluation of drying test data. **Trans. 10th Intern. Conf. on Strucutural Mechanics in Reactor Technology**, Q,71-79.